

# Mass-degenerate Heavy Vector Mesons at Hadron Colliders

Maurizio Piai and Mark Round  
Swansea University, School of Physical Sciences,  
Singleton Park, Swansea, Wales, UK  
(Dated: December 15, 2019)

We study the LHC phenomenology of a couple of mass-degenerate heavy new gauge bosons with the quantum numbers of the  $Z$  and  $\gamma$ . We give a leading-order estimate of the number of events expected in Drell-Yan processes in terms of the parameters of the model (mass and coupling) and of the LHC machine specifications (luminosity and energy). We consider the feasibility of measuring a forward-backward asymmetry for various choices of the parameters and estimate the potential reach. We comment on how the results may affect future collider design and the results for a specific model of electro-weak symmetry breaking by way of example.

## I. INTRODUCTION

The main purpose of the LHC is to discover the origin of electro-weak (EW) symmetry breaking and what new physics lies at the TeV scale.

One clean signal for the LHC would be the discovery of new, higher-mass copies of the standard-model (SM) gauge fields. For such a scenario, the LHC reach in observable masses and couplings is of interest. There are theoretical motivations for such searches. Many weakly-coupled extensions of the SM gauge group yield new heavy vector fields [1], which appear also in little Higgs models [2]. Even strongly-coupled extensions, such as technicolor (TC), predict the existence of towers of heavy spin-1 fields [3].

In TC models EW symmetry is broken by a condensate, along the lines of chiral symmetry breaking in QCD. Thus these models do not contain a light elementary Higgs particle<sup>1</sup>, and so the most promising test of these models at the LHC consists of looking for higher-mass spin-1 resonances. In particular, a copy of the full  $SU(2) \times U(1)$  is realized as heavy gauge bosons. In order for precision EW constraints to be satisfied [5, 6] their masses must be nearly degenerate. This means the resonances will overlap at a collider such as the LHC.

Proton-proton collisions will scan over the energy range current data allow higher resonances to occur at once the LHC reaches its design specification. In generic models these bounds are in the 1 TeV region, but in many concrete realizations lie above the 2 – 3 TeV range [7, 8].

In this paper, we consider the scenario in which a complete set of four spin-1 copies of the SM gauge bosons with heavy degenerate masses are produced in  $pp$  collisions and detected via the decay into light leptons (muons and electrons). For simplicity, we model the decay width of these particles by assuming it to be dominated by the decay into SM fermions, hence avoiding complications (and model-dependencies) arising when including the decay into light scalars and gauge bosons. The latter are suppressed in weakly-coupled models, as well as in the large- $N$  limit of strongly coupled theories.

At LHC energies the SM background is mostly hadronic, so by looking at the neutral sector of higher resonances, the  $Z$  and  $\gamma$  type particles, we exploit the very low background for muon and electron pair production. Within these assumptions we can study the event rate (at the leading-order), and identify what portion of parameter space will be testable at the LHC, as a function of its luminosity and energy.

In the SM, a forward-backward asymmetry arises from interference terms between virtual processes with the exchange of  $Z$  and  $\gamma$ , and it is a very sizable effect even in the TeV energy range. Measuring such an effect at a hadron collider is onerous but a method and its use at the LHC was surveyed by Dittmar [9], who showed that a possible deviation of the measured asymmetry from the SM prediction is a possible signature of the presence of a new, very broad resonance with the quantum numbers of a  $Z'$ .

When considering a narrow resonance (a weakly-coupled new  $Z'$ ), with mass above  $\sim 1$  TeV, the number of events in excess of the SM in the region of the resonance is so big that the study of the dilepton invariant-mass distribution provides a clear signature for discovery. For all practical purposes, the SM contribution can be ignored. In this case, one expects no significant asymmetry to be measurable, when restricting the analysis to events near the peak.

Conversely, if such a narrow peak is discovered in the data, but it results from the existence of a  $\gamma'$ , in addition to the  $Z'$  considered by Dittmar, then the interference between these two new states yields a large asymmetry. Measuring this asymmetry is hence a clean way to identify the presence of two distinct particles in the peak region, with masses so close together that they cannot be resolved in the invariant-mass distributions [10].

After providing a model-independent study of event rate and asymmetry, we apply these results to a specific model. Individual models give relations between the free parameters of the model-independent analysis and restrict the parameter space, so they are a useful illustration of the main ideas of this work.

## II. PARTON-LEVEL PROCESSES

We model the new neutral resonances by adding an extra set of  $SU(2) \times U(1)$  gauge fields into the SM electro-weak Lagrangian. We assume that some mechanism sponta-

<sup>1</sup> In some strongly coupled models, with approximate conformal symmetry, a light dilaton might be present with interactions very similar to the Higgs of the SM [4]. We do not consider this possibility.

neously breaks the  $SU(2)^2 \times U(1)^2$  gauge symmetry to the SM  $SU(2)_L \times U(1)_Y$  above the TeV scale, and that in the process a copy of the  $W$ ,  $Z$  and  $\gamma$  acquires a common mass  $m$ . We also assume that the couplings of the heavy gauge bosons to the SM currents can be written as  $Rg_{SM}$ , where  $g_{SM}$  stands for the coupling of the  $W$ ,  $Z$  and  $\gamma$ . The common mass,  $m$ , and the coupling ratio  $R$  are the only parameters.

We will need the function  $P_V$ ,

$$P_V = (\hat{s} - m^2 + im\Gamma_V)^{-1}, \quad (1)$$

where  $V = \gamma', Z'$ , which enters the propagator of the boson  $V$ . Note that this requires computing the decay widths for the two new resonances. In a model with extra neutral resonances, decay to SM bosons (e.g.  $Z' \rightarrow W^+W^-$ ) becomes possible. However the rate of such processes is very model-dependent, and at the same time assuming it to dominate the decay width might imply that the model be strongly coupled. In this study we assume such channels are negligible. This is equivalent to setting the 3-point and 4-point vertices to zero. If the underlying dynamics is the one of a large- $N$  gauge theory, and the heavy spin-1 states are mesons of the strongly coupled sector analogous to the  $\rho$  and  $a_1$  of a QCD-like theory, this assumption is justified by the  $1/N$  counting.

Immediately then the  $\gamma'$  and  $Z'$  have decay widths proportional to those of the  $\gamma$  and  $Z$  in the SM. For decay into SM fermions the widths are,

$$\Gamma_{\gamma'} = \frac{8}{3} R \alpha m, \quad (2)$$

$$\Gamma_{Z'} = \frac{Rg^2m}{4\pi \cos^2 \theta_w} \left( 1 - 2 \sin^2 \theta_w + \frac{8}{3} \sin^4 \theta_w \right), \quad (3)$$

where we summed over all the SM fermions, including the top and neglecting the masses. As an illustration of the model, let's remove the complications of  $pp$  collisions and take the case of  $e^+e^- \rightarrow \mu^+\mu^-$ . There are four possible diagrams; in addition to the SM channels of  $\gamma$  and  $Z$  exchange there is also  $\gamma'$  and  $Z'$ . Introducing  $c_V$  and  $c_A$  for the vector and axial couplings defined as,

$$c_V \equiv T^3 - 2Q \sin^2 \theta_w, \quad (4)$$

$$c_A \equiv T^3, \quad (5)$$

where  $Q$  denotes the particle charge, and the tree-level cross-section follows.

The new resonances behave much like their SM cousins, thus we denote

$$\Pi_\gamma(\hat{s}) = 4\pi\alpha Q_i Q_f (P_\gamma + R P_{\gamma'}), \quad (6)$$

$$\Pi_Z(\hat{s}) = \frac{g^2}{4 \cos^2 \theta_w} (P_Z + R P_{Z'}). \quad (7)$$

The  $2 \rightarrow 2$  partonic cross-section is

$$\frac{d^2 \hat{\sigma}}{d\hat{\Omega}} = \kappa \left\{ A(1 + \cos^2 \hat{\theta}) + B \cos \hat{\theta} \right\}, \quad (8)$$

where  $\kappa$  involves the parton centre of mass energy  $\hat{s}$

$$\kappa = \frac{\hat{s}}{64\pi^2}, \quad (9)$$

and

$$A = |\Pi_\gamma|^2 + 2c_V^2 \Re(\Pi_\gamma \Pi_Z^*) + (c_V^2 + c_A^2)^2 |\Pi_Z|^2 \quad (10)$$

$$B = 4c_A^2 \Re(\Pi_\gamma \Pi_Z^*) + 8c_V^2 c_A^2 |\Pi_Z|^2 \quad (11)$$

The forward-backward asymmetry  $A_{FB}$  is

$$A_{FB} = \frac{\left( \int_0^1 - \int_{-1}^0 \right) d \cos \hat{\theta} d\sigma / d \cos \hat{\theta}}{\left( \int_0^1 + \int_{-1}^0 \right) d \cos \hat{\theta} d\sigma / d \cos \hat{\theta}}, \quad (12)$$

or, equivalently,

$$A_{FB} = \frac{3B}{8A}. \quad (13)$$

This result can be used to rewrite the cross-section in terms of an angular function  $g(\hat{\theta})$ :

$$\frac{d^2 \sigma}{d\Omega} = \frac{3\kappa}{8A} g(\hat{\theta}), \quad (14)$$

with

$$g(\hat{\theta}) = \frac{3}{8} (1 + \cos^2 \hat{\theta}) + A_{FB} \cos \hat{\theta}. \quad (15)$$

Above an energy of 500 GeV the SM boson contribution becomes negligible for our purposes, as anticipated in the introduction. Near the resonance,  $\hat{s} \simeq m^2$ , the new particles contribute far more than the SM ones, as long as  $m\Gamma_{V'} \ll \hat{s}$ . Since in this case

$$|P_V| \simeq \hat{s}^{-1}, \quad (16)$$

$$|P_{V'}| \simeq (m\Gamma_{V'})^{-1}, \quad (17)$$

unless  $R$  is very small the new resonances will dominate. The definitions of  $\Pi_V$  given can now be approximated by dropping the  $P_V$  terms.

$$\Pi_V \propto P_{V'}. \quad (18)$$

We use this approximation to re-write the (non-vanishing) asymmetry at the new resonance pole ( $\hat{s} = m^2$ ) as,

$$A_{FB} = \frac{3}{2} \frac{c_A^2 \Gamma_{\gamma'} \Gamma_{Z'} + 2c_V^2 c_A^2 \Gamma_{\gamma'}^2}{\Gamma_{Z'}^2 + 2c_V^2 \Gamma_{\gamma'} \Gamma_{Z'} + (c_V^2 + c_A^2)^2 \Gamma_{\gamma'}^2}. \quad (19)$$

Now we consider a hadron collider. The formulae for asymmetry and cross-section can be amended by adding a factor for the number of colors,  $N_c$ , and changing to quark couplings. Denoting the quark/lepton couplings with a  $q/l$  superscript  $A$  is modified to,

$$A_{q \rightarrow l} = |\Pi_\gamma|^2 + 2c_V^q c_V^l \Re(\Pi_\gamma \Pi_Z^*) + (c_V^{q2} + c_A^{q2})(c_V^{l2} + c_A^{l2}) |\Pi_Z|^2. \quad (20)$$

Adding in the color factor the partonic cross-section for  $q\bar{q} \rightarrow l^+l^-$  is,

$$\frac{d\hat{\sigma}}{d\hat{s}} = \frac{1}{N_c} \frac{\hat{s}}{12\pi} A_{q \rightarrow l}, \quad (21)$$

where the angular dependence has been integrated over. Adjusting  $B$  to account for quarks,

$$B_{q \rightarrow l} = 4c_A^q c_A^l \Re(\Pi_\gamma \Pi_Z^*) + 8c_V^q c_V^l c_A^q c_A^l |\Pi_Z|^2. \quad (22)$$

The asymmetry at the partonic level is hence

$$A_{FB} = \frac{3B_{q \rightarrow l}}{8A_{q \rightarrow l}}. \quad (23)$$

### III. DRELL-YAN PROCESSES

We will follow the standard recipe to model processes at a hadron collider of considering the incident protons to be composed of partons holding fractions,  $\xi$ , of the total proton momentum  $p$ . Numerous sets of parton distribution functions are available through Fortran code [11]. For this paper we choose the Fermi02 PDF set [12]. Let us begin by assuming that the proton is massless as are the constituent partons. The two beams of protons each have energy  $\sqrt{s}/2$ . The energy of a parton-parton collision,  $\hat{s}$ , is given in terms of the two fractions  $\xi_1$  and  $\xi_2$  as,

$$\hat{s} = \xi_1 \xi_2 s. \quad (24)$$

If, for a parton  $x$ , the PDF is denoted by  $f_x(\xi)$  we can follow convention and write the  $pp \rightarrow l^+ l^-$  cross-section as,

$$\frac{d^3\sigma}{d\xi_1 d\xi_2 d\hat{s}} = \sum_q [f_q(\xi_1) f_{\bar{q}}(\xi_2) + f_q(\xi_2) f_{\bar{q}}(\xi_1)] \frac{d\hat{\sigma}}{d\hat{s}}. \quad (25)$$

To fix the total energy  $\sqrt{s}$  of the  $pp$  collision, we impose the condition of Eq. (24). This means we may define  $\mathcal{L}_q$  to be

$$\begin{aligned} \mathcal{L}_q &\equiv \int_0^1 \int_0^1 \delta(\hat{s} - \xi_1 \xi_2 s) [f_q(\xi_1) f_{\bar{q}}(\xi_2) + \xi_1 \leftrightarrow \xi_2] d\xi_1 d\xi_2, \\ &= \frac{2}{s} \int_{\hat{s}/s}^1 \frac{1}{\xi} f_q(\xi) f_{\bar{q}}\left(\frac{\hat{s}}{s\xi}\right) d\xi \end{aligned} \quad (26)$$

and write the full cross-section summed over all quarks as,

$$\frac{d\sigma}{d\hat{s}} = \sum_q \frac{d\hat{\sigma}}{d\hat{s}} \mathcal{L}_q. \quad (27)$$

Finally we can write the total number of events,  $N$  in some range of  $\hat{s}$  at a machine luminosity  $L$ ,

$$N = L \int \frac{d\sigma}{d\hat{s}} d\hat{s}. \quad (28)$$

We allow  $\sqrt{s}$  to vary between 10 and 28 TeV. The coupling ratio,  $R$ , will be taken as between 0 and 1 where the theory is certainly perturbative. Then the mass range will be taken as lying between 1 and 4 TeV. Analysis will also frequently require the assumption that decay widths are small compared to the resonance mass. Inspection of the decay widths, under the limits on  $R$  and  $m$ , shows this condition will be satisfied.

Asymmetry measurements at a hadron collider are made more difficult (in comparison with a leptonic machine) by the unknown direction of the initial quark (anti-quark). However, at high rapidity there is a much greater chance that the quark carries the bulk of the momentum as opposed to the alternative. Thus if the data from a peak were to be cut so that only events with a rapidity  $Y$  greater than some cut value  $Y_c$  ( $|Y| > Y_c$ ) are used, then there is a corresponding degree of certainty regarding the quark direction. This method is used and explained more fully by Dittmar [9]. In summary though, the magnitude of the rapidity controls the uncertainty in the quark direction, while the sign of the rapidity represents whether the quark was from the left or right in the collider. This methodology of inserting cuts, Lorentz boosting with the rapidity modulus to the muon centre of mass frame and finally the sign of  $Y$  to define the angle consistently allows one to infer an asymmetry. Such an asymmetry is the remnant of the partonic asymmetry.

### IV. MODEL INDEPENDENT STUDY

#### A. Event Rate

In this section, we introduce a set of approximations that are useful in order to study the dependence of observable quantities (such as number of expected events and forward-backward asymmetry) on the parameters of the model and on the machine specifications. The numerical part of the analysis will, however, use the complete equations and PDF distributions without approximations.

Using standard electro-weak relations the coupling  $g$  can be written in terms of  $\alpha$  and  $\sin^2 \theta_w \simeq 0.22$ . Hence, near the new resonance:

$$\frac{\Pi_\gamma}{\Pi_Z} \simeq -\frac{3}{2} Q_q \left( 1 - 2 \sin^2 \theta_w + \frac{8}{3} \sin^4 \theta_w \right) \simeq -Q_q. \quad (29)$$

Using now Eqs. (20)-(21) we can comment on the relative strength of the  $\gamma'$  and  $Z'$  contributions to the total cross-section. Because  $c_v^l \ll 1$ , the cross term in Eq. (21) is suppressed. Also, in the last term of this equation  $c_V^{f2} \ll c_A^{f2} \simeq 1/4$ , and hence the contribution of the  $\gamma'$  is a factor of  $16Q_q^2$  larger than the contribution coming from the  $Z'$ . All of this, together with the fact that the PDF for the up-quark and down-quarks are the most important, and that the coupling of the up quarks to  $\gamma'$  is four times stronger than the coupling of down quarks, means that the most significant contribution to the total event rate is given by the subprocess  $u\bar{u} \rightarrow \gamma' \rightarrow \mu^+ \mu^-$ .

Focusing on the  $u$ -quark PDF we may attempt to approximate it with some form of expansion. The only relevant dimensionless combination is  $\hat{s}/s$  and from the definition of  $\mathcal{L}$  the overall dimension is  $1/s$ . If the mass of the resonance were to increase one would expect the event rate to decrease. The mass is the peak location, which is synonymous with  $\hat{s}$ . It is also reasonable to think increasing the machine energy  $s$  will

increase the event rate so,

$$\mathcal{L}_u \sim \frac{1}{s} \left( \frac{\hat{s}}{s} \right)^n, \quad (30)$$

should obey these criteria. The minimal  $n$  would be  $-2$ . Viewing this as the first term in some expansion a polynomial can be added to increase accuracy. We can argue the nature of this polynomial by considering the limiting behaviour. As  $s \rightarrow 0$  the luminosity should vanish while the expansion parameter will blow-up thus we can say,

$$\mathcal{L}_u \sim \frac{s}{\hat{s}^2} \cdot \frac{1}{1 + a_1(\hat{s}/s)^2 + a_2(\hat{s}/s)^4 + \dots}, \quad (31)$$

for  $\sqrt{\hat{s}} \in [1, 4]$  TeV. We then go through a numerical fit of the constants  $a_1$  and  $a_2$ . In the range  $\sqrt{\hat{s}} \in [10, 28]$  TeV just those two terms are needed.

We are interested in the event rate  $N$  in the peak region

$$\begin{aligned} N &\propto \int \sum_q \frac{d\sigma}{d\hat{s}} d\hat{s}, \\ &\simeq \int \mathcal{L}_u \frac{d\hat{\sigma}_u}{d\hat{s}} d\hat{s}. \end{aligned} \quad (32)$$

Approximating  $\mathcal{L}_u$  with its value at the pole (which is allowed since the resonances are very narrow), and using

$$\int \frac{\hat{s}}{(\hat{s} - m^2)^2 + m^2 \Gamma_{\gamma'}^2} d\hat{s} \simeq 2\pi \frac{m}{\Gamma_{\gamma'}}. \quad (33)$$

yields

$$\int \mathcal{L}_u \frac{d\hat{\sigma}_u}{d\hat{s}} d\hat{s} \simeq \mathcal{L}_u(m^2) R^2 2\pi \frac{m}{\Gamma_{\gamma'}} \quad (34)$$

$$\propto R \mathcal{L}_u(m^2), \quad (35)$$

where effectively the SM background from  $\gamma$  and  $Z$  has been neglected.

Finally, the contribution of up-quarks to the total rate is,

$$N_u \propto \frac{sLR}{m^4} \cdot \frac{1}{1 + a_1 m^4/s^2 + a_2 m^8/s^4}, \quad (36)$$

up to a proportionality constant that contains the electro-weak couplings and the normalization of the PDF distribution.

To correct for the neglected contributions of  $d\bar{d}$  events and  $Z'$  exchange we can consider the ratio of the found rate  $N_u$  to a more complete expression involving  $u\bar{u}$  and  $d\bar{d}$  events with  $\gamma'$  and  $Z'$  exchange. For notational simplicity let us absorb the coupling coefficients into the definition of  $P_V$  briefly and write the ratio  $\eta$  as,

$$\frac{1}{\eta} \equiv \frac{\mathcal{L}_u \int \hat{s} |P_{\gamma'}|^2 d\hat{s}}{\mathcal{L}_u \int \hat{s} |P_{\gamma'} + P_{Z'}|^2 d\hat{s} + \mathcal{L}_d \int \hat{s} |P_{\gamma'} + P_{Z'}|^2 d\hat{s}}. \quad (37)$$

An expression similar to Eq. (31) describes, with different choices of the coefficients,  $\mathcal{L}_d$ . Then we find that a very good approximation is given by

$$\frac{1}{\eta} = \frac{1 + b_1(\hat{s}/s)^2 + b_2(\hat{s}/s)^4}{1 + a_1(\hat{s}/s)^2 + a_2(\hat{s}/s)^4} (1 + c_1 m + c_2 R) \quad (38)$$

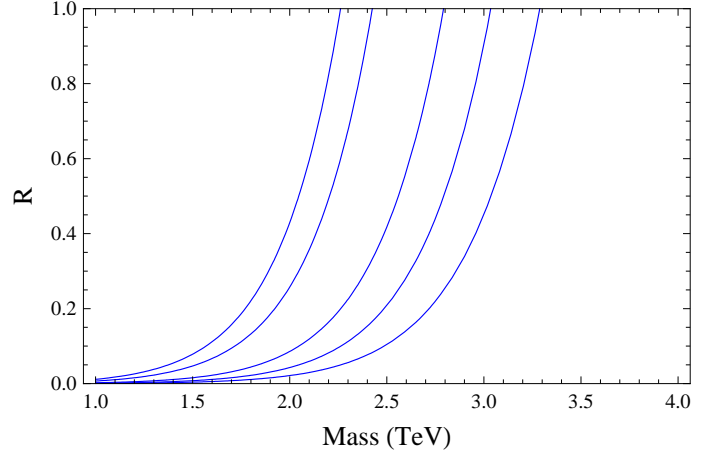


FIG. 1: The minimal coupling  $R$  for various choices of the event number  $N$  divided by the luminosity  $L$  at  $\sqrt{s} = 10$  TeV. From the left,  $N/L = 5, 3, 1, 1/2, 1/4$  fb.

for some  $b_i$  and  $c_i$  that are combinations of the up and down coefficients.

The total event rate can be written, up to an overall constant, as

$$N \simeq N_u \eta. \quad (39)$$

We fix the parameters,  $a_1, a_2, b_1, b_2, c_1, c_2$  plus an overall normalisation with the direct numerical computation using the PDFs. We estimate the error hence introduced between the estimated event rate and the direct computation to be about 5%.

Discovery of the new resonance depends on some value of the ratio  $N/L$  of the event number  $N$  and the machine luminosity  $L$ . The approximate event rate can be solved for  $R$  given  $m$  at various machine energies and luminosities producing Figs. 1 and 2. These two plots show how improving the energy of a hadron collider compared to increasing the luminosity affects the search.

Take the  $N/L = 3$  fb curve. If one were to triple the luminosity of the machine that would imply moving to the next curve on the right. However if one were to improve the machine energy from 10 TeV to 24 TeV that would mean moving from Fig. 1 to Fig. 2. By improving the luminosity by a factor of 20, one may move from a reach in masses below 2.2 TeV to roughly 3.3 TeV at a 10 TeV machine. Whilst improving the collision energy takes the reach to well above 4.0 TeV, even at low luminosity.

## B. Forward-Backward Asymmetry

We restrict our attention to two main sources of error in the asymmetry extraction algorithm. We set aside experimental errors, coming for instance from the measurement of the energy of the final leptons, and instead we estimate the statistical error from general statistics considerations, such as the use of a sample of  $N$  events to model a distribution.

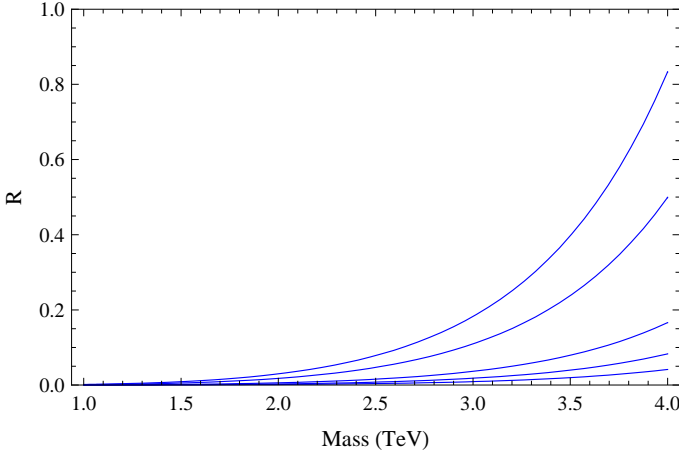


FIG. 2: The minimal coupling  $R$  for various choices of the event number  $N$  divided by the luminosity  $L$  at  $\sqrt{s} = 24$  TeV. From the left,  $N/L = 5, 3, 1, 1/2, 1/4$  fb.

Consider the angular distribution in Eq. (15) as a probability distribution function. This distribution has a mean defined as

$$\langle \hat{\theta} \rangle = \int \hat{\theta} g(\hat{\theta}) \sin \hat{\theta} d\hat{\theta} = \frac{\pi}{4} (2 - A_{FB}), \quad (40)$$

while

$$\sigma_p^2 \equiv \int (\hat{\theta}^2 - \langle \hat{\theta} \rangle^2) g(\hat{\theta}) \sin \hat{\theta} d\hat{\theta}. \quad (41)$$

Interestingly,  $A_{FB}$  turns out to be just proportional to  $\langle \hat{\theta} \rangle$ . Hence we can estimate the statistical error on the extraction of the symmetry as

$$\Delta A_{FB}^{\text{stat}} = \frac{4\sigma_p}{\pi\sqrt{n-1}}, \quad (42)$$

where  $n$  is the number of events used to study the angular distribution.

Secondly there is an error introduced by the methodology. The assumption that the initial quark direction be always the one of the outgoing  $\gamma'$  of  $Z'$ , implies a possible misidentification  $\hat{\theta} \leftrightarrow \pi - \hat{\theta}$ . Let the probability of mis-identification be  $p$ , then in a sample of  $n$  events  $np$  are mis-identified. Let  $n_F$  ( $n_B$ ) events travel in the forward (backward) direction. Then  $n = n_F + n_B$ . The worst case scenario would be that all  $np$  events were placed in  $n_F$  but should have been placed in  $n_B$ . In this case the difference in true and measured asymmetry would be,

$$\Delta A_{FB}^{\text{sys}} = \pm 2p \quad (43)$$

This means that adding the method and statistical errors together the total error will be,

$$\Delta A_{FB} = \frac{4\sigma_p}{\pi\sqrt{n-1}} + 2p(Y_c), \quad (44)$$

where the dependence of  $p$  on the cut  $Y_c$  has been added for clarity. We conservatively add the two sources of error linearly.

Now we can define  $P(Y_c)$ , the fraction of events with  $|Y| > Y_c$ . Then, the number of events used to extract the asymmetry is,

$$n = PN. \quad (45)$$

Requiring that  $\Delta A_{FB} < \mathcal{E}$  (for  $\mathcal{E} > 2p$ ) implies

$$n > \left( \frac{4\sigma_{pop}}{\pi(\mathcal{E} - 2p)} \right)^2 + 1 \quad (46)$$

or equivalently,

$$N > \frac{1}{P} \left[ \left( \frac{4\sigma_{pop}}{\pi(\mathcal{E} - 2p)} \right)^2 + 1 \right] \quad (47)$$

total events.

For the model considered, at the partonic level the asymmetry is  $A_{FB} \simeq -0.5$  in the case of  $u\bar{u} \rightarrow \mu^+\mu^-$ , while for  $d\bar{d}$  events the asymmetry would be  $A_{FB} \simeq -0.15$ . (For comparison, SM exchange plus only one new resonance the asymmetry vanishes up to 3 decimal places.) The measured asymmetry will then be some average of the two. Using what we showed before, namely that the  $u\bar{u}$  events give a larger contribution to the total rate, we estimate the combined asymmetry to be  $A_{FB} \sim -0.42$ . Therefore seeing an asymmetry at a collider would indicate that there are two particles in the new neutral resonance.

To measure such an effect at a collider one would require an error  $\mathcal{E} < 0.14$  in order to conclude, at the  $3\sigma$  level, an asymmetry is present. Consider the case that all events happen to fall precisely at the rapidity cut  $Y_c$ . Then the probability  $p$  is calculable, yielding a conservative estimate: with real data having  $|Y| > Y_c$  in general the error probability will be smaller than this  $p$ . The fraction  $P$  can also be computed. This is also an estimate as it is open to a sampling error just as the asymmetry measure is. However this error will be neglected as for  $3\sigma$  measurements the number of events required is large, typically hundreds.

Optimal choice of  $Y_c$  for a minimal  $N$  can be achieved by writing a simple minimisation algorithm. A high  $Y_c$  gives high quality data (i. e. contaminated by small misidentification systematics) with low  $p$  but few events will pass such a cut, reducing also  $P$ . The converse will be true for a low cut  $Y_c$ . We used an optimisation algorithm finding a  $Y_c$  such that the required number of events has been minimised.

Once the minimum event number has been determined, yielding the required  $3\sigma$  error on the asymmetry measurement for a given mass, the associated minimal coupling  $R$  can be estimated from the approximate event rate in Eqs. (38) and (39). The results of this process are shown in Figs. 3 and 4. Figure 3 shows that large increases in luminosity lead to modest gains in reach, compared to the gain obtained by going to larger energies, as shown in Fig. 4.

## V. PDF ERROR

So far the error on the PDFs themselves has been completely ignored. The Fortran module supplied by [11] has the capability to compute PDF errors. As the computational cost to produce errors is very large, we used an approximate expression which captures the essential features of the PDF errors. Namely, the quark PDFs are well known up to fractions of around 0.5, then they become poorly understood while the anti-quark PDFs are poorly understood across all of the fraction range. Two piecewise functions, one for the  $u$  and one for the  $\bar{u}$ , approximate this behavior

$$\frac{\Delta u(\xi)}{u(\xi)} = \begin{cases} 0.05 & \text{if } \xi < 0.5 \\ 0.8\xi - 0.35 & \text{otherwise} \end{cases} \quad (48)$$

$$\frac{\Delta \bar{u}(\xi)}{\bar{u}(\xi)} = \begin{cases} 2.25\xi & \text{if } \xi < 0.8 \\ 25\xi - 18.2 & \text{otherwise} \end{cases} \quad (49)$$

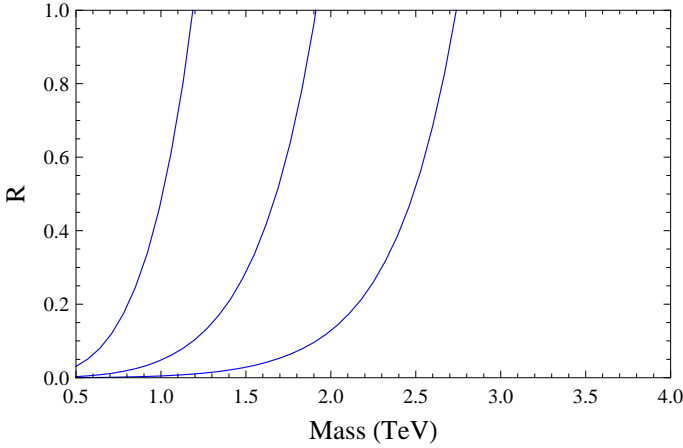


FIG. 3: Minimal coupling  $R$ , as a function of the mass  $m$ , required to observe a  $3\sigma$   $A_{FB} \sim -0.42$  at the resonance for  $L = 1, 10, 100 \text{ fb}^{-1}$  and a  $\sqrt{s} = 14 \text{ TeV}$  hadron collider.

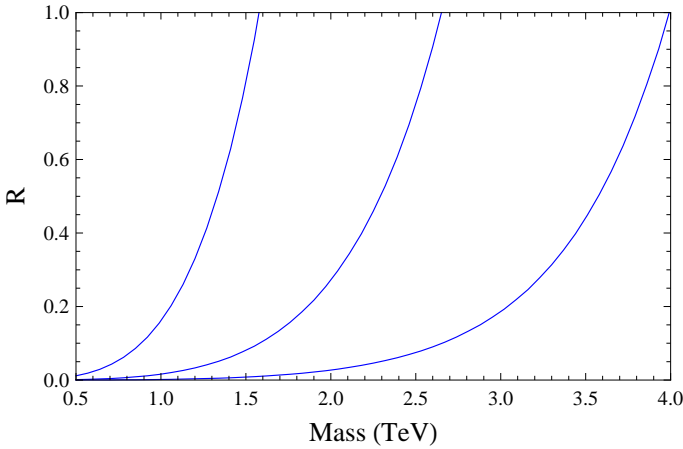


FIG. 4: Minimal coupling  $R$ , as a function of the mass  $m$ , required to observe a  $3\sigma$   $A_{FB} \sim -0.42$  at the resonance for  $L = 1, 10, 100 \text{ fb}^{-1}$  and a  $\sqrt{s} = 24 \text{ TeV}$  hadron collider.

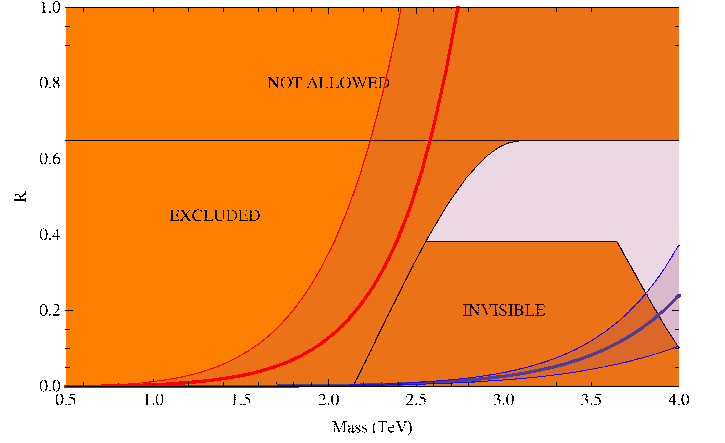


FIG. 5: Discovery reach at  $\sqrt{s} = 14 \text{ TeV}$  for the specific model in the text, at  $L = 100 \text{ fb}^{-1}$ . The red line represents the  $3\sigma$   $A_{FB}$  discovery (neglecting PDF uncertainties), with a  $1\sigma$  error from the PDFs represented by shading. The blue represents the critical 10 events observed with the  $1\sigma$  error from the PDF added through shading.

These errors broadly agree with those published by the CTEQ group for their PDF sets [13]. Even if an event is not identified as being  $u\bar{u}$  or  $d\bar{d}$  in our analysis, the former dominates and hence the error indicated will offer a good guide as to the situation.

As the asymmetry extraction methodology involves cutting the data for large  $Y$ , it probes the region with a smaller anti-quark fraction and a larger quark fraction. If the quark fraction gets above 0.5 the error grows rapidly. At a 10 TeV collider this effect will come in faster as high fractions are required to make large invariant masses while the effect will be slower to appear in a 24 TeV collider.

Most events will occur with low rapidity. As a result we expect far lower errors on event rate measurements compared to asymmetry measurements.

## VI. AN EXAMPLE MODEL

In order to illustrate the results of the model-independent study, it is useful to apply them to a specific model. For example in the AdS/TC model [14] a 5D model is formulated in AdS space and bounds on the  $(R, m)$  parameter space discussed.

Several qualitatively different regions of the  $(R, m)$  parameter space are identified. Firstly there is a region where the dominant decay mode of the techni- $\rho$  particles is into SM gauge bosons, and not SM fermions. This region is marked as *invisible* because the branching ratio into fermions would strongly suppress the Drell-Yan process of interest here. There is then a second region already *excluded* by precision measurements. Finally the constraint  $R \lesssim 0.65$  comes from specific details of the model.

Putting this information into a plot and overlaying the search capabilities of a collider produces Figs. 5 and 6. At

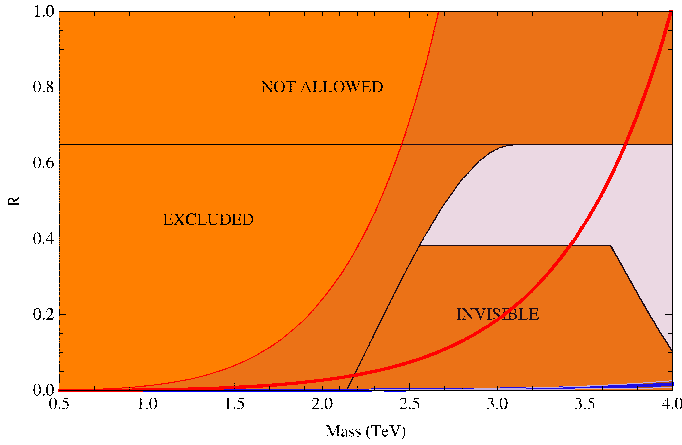


FIG. 6: Discovery reach at  $\sqrt{s}=24$  TeV for the specific model in the text, at  $L = 100 \text{ fb}^{-1}$ . The red line represents the  $3\sigma$   $A_{FB}$  discovery (neglecting PDF uncertainties), with a  $1\sigma$  error from the PDFs represented by shading. The blue represents the critical 10 events observed with the  $1\sigma$  error from the PDF added through shading.

the very high luminosity of Fig. 5 most of the parameter space will be tested for the existence of new resonances. However, there is no reach in terms of asymmetry. Thus it will be hard to conclude whether there is more than one particle responsible for the peak. In contrast, with the higher collision energy of Fig. 6, more than half the parameter space presents a testable asymmetry.

Both Figs. 5 & 6 include a  $1\sigma$  PDF error through shading. It is clear that the event rate error is much smaller in the 24 TeV case with the cone barely visible on the plot. As for the asymmetry, the error at 14 TeV grows much faster for those masses where the 14 and 24 TeV lines are both able to reach. In the case of the 14 TeV curve, the error in coupling is 10 times the coupling estimate by 2 TeV. In comparison the coupling error will not reach a factor of 10 until 3.5 TeV in the 24 TeV machine.

For the representative point  $m = 2.6$  TeV and  $R = 0.4$  we simulate the asymmetry and see the rapidity cut in action. For simplicity, we assume that only  $u\bar{u}$  events contribute at the partonic level. As explained, this is the dominant subprocess, although as a check simulations including  $d\bar{d}$  were run which confirmed expectations or lowering the asymmetry mildly. In this limit, the asymmetry is  $A_{FB} \simeq -0.5$ .

First let us look at the events with  $\sqrt{s} = 24$  TeV. We apply a cut rapidity  $Y > Y_c = 1.0$ . In this way the systematic error due to the methodology is relatively small ( $\simeq 0.1$ ). Also, the number of events that pass the cut is large enough as to make the statistic error very small ( $\sim 0.03$ ). As a result, the simulated set plotted in Fig 7 clearly shows a large asymmetry, compatible with the true one, and  $\sim 4\sigma$  away from zero.

By comparison, in Fig. 8 we show a set of simulated events with the same choices of parameters, but  $\sqrt{s} = 14$  TeV. In this case we apply a lower cut of  $Y > Y_c = 0.75$ . As a result, the asymmetry of the simulated data is  $A_{FB} = -0.45 \pm 0.07(\text{stat}) \pm 0.14(\text{sys})$ , lower than the expected true

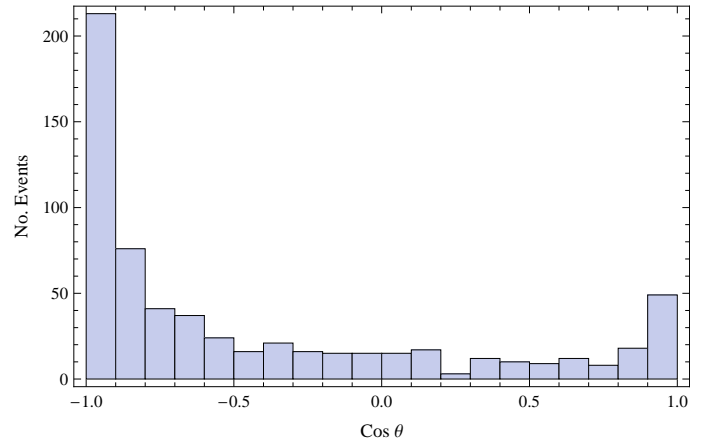


FIG. 7: Simulated center of mass angle distribution at  $\sqrt{s}=24$  TeV, and  $L = 100 \text{ fb}^{-1}$ , for  $m = 2.6$  TeV and  $R = 0.4$  restricted to rapidity  $Y > Y_c = 1.0$ . The resulting asymmetry is  $A_{FB} = -0.51 \pm 0.03(\text{stat}) \pm 0.1(\text{sys})$ .

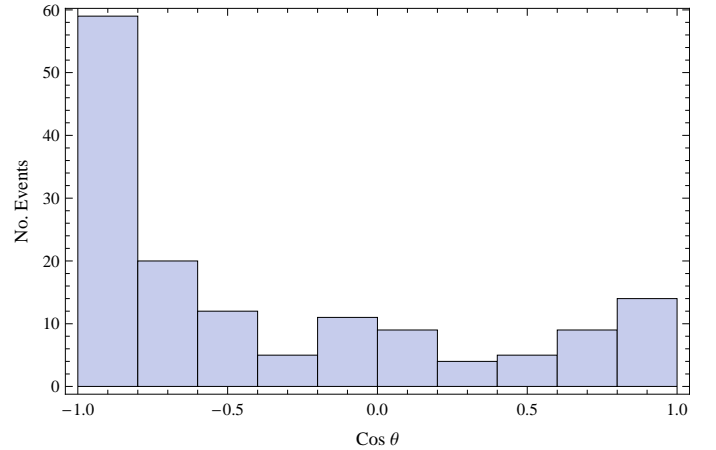


FIG. 8: Simulated center of mass angle distribution at  $\sqrt{s}=14$  TeV, and  $L = 100 \text{ fb}^{-1}$ , for  $m = 2.6$  TeV and  $R = 0.4$  restricted to rapidity  $Y > Y_c = 0.75$ . The resulting asymmetry is  $A_{FB} = -0.45 \pm 0.07(\text{stat}) \pm 0.14(\text{sys})$ .

value, and affected by large uncertainties.

A final comment is in order. In this numerical analysis we did not take into account the effect of experimental errors, and in particular of the kinematical cuts that might be applied to extract the events to be analyzed. For example, when  $|\cos \theta| \simeq 1$  the experimental extraction of the kinematics of the two final leptons might be problematic. In order to understand how important this effect is, we extracted the asymmetry from the simulated data by imposing the further constraint  $|\cos \theta| < 0.8$ . This procedure effectively reduces the forward-backward asymmetry to  $A_{FB} = -0.37$  ( $A_{FB} = -0.28$ ) in the 24 (14) TeV case. This reduction can be thought of as a further systematic error, coming from the fact that Eq. (23) should be modified integrating only over a limited range of  $\theta$ .

These two examples show how the method works out in practice. However caution must be noted that in perform-



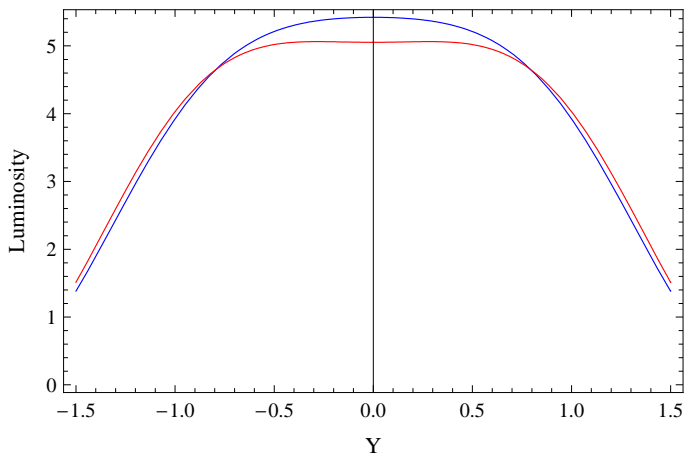


FIG. 9: The expected rapidity distribution for a pure  $Z'$  (blue) and a pure  $\gamma'$  (red) for a 2.6 TeV mass at a  $\sqrt{s} = 24$  TeV collider, assuming same number of events.

ing such simulations there is a great degree of sensitivity to choice of PDF sets and computational noise. We illustrate here that the method functions but very different results may be obtained depending on how the large- $\xi$  distributions are modelled, and ultimately this problem will be resolved only once actual data are collected.

## VII. NON-DEGENERATE COUPLINGS

The region at low rapidity exhibits an interesting feature. Due to the differences in the up and down PDF distributions, the rapidity distributions of these two types of partonic events have very distinct shapes: up-type events peak at finite  $Y$ , while down-type peak at  $Y = 0$ . In principle, this might allow to discriminate between different values of the couplings  $R_{\gamma'}$  and  $R_{Z'}$  of the new resonances to the up and down quarks.

To investigate the feasibility of such a measurement we examine the two extreme cases, that  $R_{\gamma'} = 0$  versus  $R_{Z'} = 0$ . We normalize the distributions to the same area, hence fixing the event number. The result is shown in Fig. 9. We see the largest effect is around  $Y = 0$  where there is a 1 part in 25 difference, or 5%. The chosen situation is the most extreme, a light mass in terms of what the precision constraints allow and a high energy collider. We can conclude that the effect of a non-degenerate  $R$  will be so small as not to be measurable, even assuming perfect detector efficiency and no kinematic cuts.

## VIII. CONCLUSIONS

We performed a model-independent study of the Drell-Yan processes at the LHC, assuming that two new gauge bosons with quantum numbers and couplings analogous to the photon and  $Z$  boson, but rescaled by a common factor of  $R < 1$ , have masses so close to each other that their kinematic peaks are

indistinguishable.

We assumed perfect detector performance, not including experimental errors, such as energy resolution, and without including the effect of kinematical cuts. We did not include any QCD corrections to the tree-level partonic calculation of  $pp \rightarrow \mu^+\mu^-$  and  $pp \rightarrow e^+e^-$ . In relation to the forward-backward asymmetry, we included in the analysis the main sources of theoretical error: a statistical error related to the number of expected events, a systematic error due to the misidentification of the direction of the initial (anti-)quark, and the uncertainty due to the PDF distributions.

The results can be interpreted as a best case scenario at the LHC, limited only by theoretical considerations. We compared different choices of the luminosity and center-of-mass energy of the  $pp$  collisions. For illustration purposes, we also referred to one specific model, in which such mass-degenerate, weakly-coupled new gauge bosons are required by imposing the bounds on precision electro-weak parameters.

For a 10 TeV collider, and luminosities in the  $2 - 40\text{fb}^{-1}$ , bounds on new resonances no higher than 3 TeV can be obtained. With a 24 TeV collider the region well over 4 TeV can be explored, depending on the specific coupling  $R$ . The error imparted upon this prediction from the PDFs is quite modest for a high energy collider, while at lower energies, like 10 TeV, the PDF uncertainty at large momentum fraction is an important limiting factor.

As for the forward-backward asymmetry. The collider ability to measure an asymmetry at the  $3\sigma$  level is heavily restricted to light masses. Even at very high luminosities measuring the asymmetry for masses of 3 TeV is out of reach for a 14 TeV collider, even in principle. Factoring in the PDF error, it is hard to conceive of any possible asymmetry measurements in a 14 TeV collider. By contrast, at a 24 TeV machine the PDF error is markedly lower and the reach far larger. At such a machine it may be possible to measure asymmetries and greatly restrict currently open parameter spaces.

Measuring the forward-backward asymmetry in this class of events provides a theoretically clean signal allowing one to discriminate the presence of more than one neutral gauge boson in a heavy resonance. Such a measurement is very difficult in practice, and the effect of large PDF uncertainties at large momentum fraction, together with the scaling of event rate with  $s$ , suggests upgrading the LHC to a higher energy (besides increasing the luminosity), if, as is the case in many phenomenological models, the precise features of new, very heavy gauge bosons are of interest.

## Acknowledgments

We would like to thank S. de Curtis and M. Fabbrihesi for useful discussions. The work of MR is supported by the STFC Doctoral Training Grant ST/F00706X/1. The work of MP is supported in part by the Wales Institute of Mathematical and Computational Sciences and by the STFC Grant ST/G000506/1.



- 
- [1] See for instance T. Appelquist, B. A. Dobrescu and A. R. Hopper, Phys. Rev. D **68**, 035012 (2003) [arXiv:hep-ph/0212073], and references therein.
- [2] See for instance N. Arkani-Hamed, A. G. Cohen, E. Katz and A. E. Nelson, JHEP **0207**, 034 (2002) [arXiv:hep-ph/0206021]; I. Low, W. Skiba and D. Tucker-Smith, Phys. Rev. D **66**, 072001 (2002) [arXiv:hep-ph/0207243].
- [3] S. Weinberg, Phys. Rev. D **19**, 1277 (1979); L. Susskind, Phys. Rev. D **20**, 2619 (1979); S. Weinberg, Phys. Rev. D **13**, 974 (1976).
- [4] W. A. Bardeen, C. N. Leung and S. T. Love, Phys. Rev. Lett. **56**, 1230 (1986); M. Bando, K. i. Matumoto and K. Yamawaki, Phys. Lett. B **178**, 308 (1986); B. Holdom and J. Terning, Phys. Lett. B **187**, 357 (1987), Phys. Lett. B **200**, 338 (1988); W. D. Goldberger, B. Grinstein and W. Skiba, Phys. Rev. Lett. **100**, 111802 (2008) [arXiv:0708.1463 [hep-ph]].
- [5] M. E. Peskin and T. Takeuchi, Phys. Rev. D **46**, 381 (1992).
- [6] R. Barbieri, A. Pomarol, R. Rattazzi and A. Strumia, Nucl. Phys. B **703**, 127 (2004) [arXiv:hep-ph/0405040].
- [7] J. Hirn and V. Sanz, Phys. Rev. Lett. **97**, 121803 (2006) [arXiv:hep-ph/0606086], JHEP **0703**, 100 (2007) [arXiv:hep-ph/0612239]; D. K. Hong and H. U. Yee, Phys. Rev. D **74**, 015011 (2006) [arXiv:hep-ph/0602177]; M. Piai, arXiv:hep-ph/0608241, arXiv:hep-ph/0609104, arXiv:0704.2205 [hep-ph]; C. D. Carone, J. Erlich and J. A. Tan, arXiv:hep-ph/0612242; M. Fabbrichesi, M. Piai, L. Vecchi arXiv:0804.0124 [hep-ph]; K. Haba, S. Matsuzaki and K. Yamawaki, arXiv:0804.3668 [hep-ph]; J. Hirn, A. Martin and V. Sanz, arXiv:0807.2465 [hep-ph]; D. D. Dietrich and C. Kouvaris, arXiv:0809.1324 [hep-ph].
- [8] For bounds in the context of the Randall-Sundrum models, see for instance C. Csaki, J. Erlich and J. Terning, Phys. Rev. D **66**, 064021 (2002) [arXiv:hep-ph/0203034]; K. Agashe, R. Contino, L. Da Rold and A. Pomarol, Phys. Lett. B **641**, 62 (2006) [arXiv:hep-ph/0605341]; M. S. Carena, E. Ponton, J. Santiago and C. E. M. Wagner, Nucl. Phys. B **759**, 202 (2006) [arXiv:hep-ph/0607106]; Phys. Rev. D **76**, 035006 (2007) [arXiv:hep-ph/0701055]; C. Bouchart and G. Moreau, Nucl. Phys. B **810**, 66 (2009) [arXiv:0807.4461 [hep-ph]]; K. Agashe *et al.*, Phys. Rev. D **76**, 115015 (2007) [arXiv:0709.0007 [hep-ph]].
- [9] M. Dittmar, Phys. Rev. D **55**, 161 (1997) [arXiv:hep-ex/9606002].
- [10] E. Accomando, S. De Curtis, D. Dominici and L. Fedeli, arXiv:0807.5051 [hep-ph].
- [11] M. R. Whalley, D. Bourilkov and R. C. Group, arXiv:hep-ph/0508110.
- [12] W. T. Giele, S. A. Keller and D. A. Kosower, arXiv:hep-ph/0104052.
- [13] J. Pumplin, D. R. Stump, J. Huston, H. L. Lai, P. M. Nadolsky and W. K. Tung, JHEP **0207**, 012 (2002) [arXiv:hep-ph/0201195].
- [14] M. Piai, arXiv:0704.2205 [hep-ph];